ACS Infectious Diseases

pubs.acs.org/journal/aidcbc

Article

Interaction of *Staphylococcus aureus* and Host Cells upon Infection of Bronchial Epithelium during Different Stages of Regeneration

Laura M. Palma Medina, Ann-Kristin Becker, Stephan Michalik, Kristin Surmann, Petra Hildebrandt, Manuela Gesell Salazar, Solomon A. Mekonnen, Lars Kaderali, Uwe Völker,* and Jan Maarten van Dijl*

Cite This: *ACS Infect. Dis.* 2020, 6, 2279−2290

Read Online

ACCESS | Metrics & More | Article Recommendations | Supporting Information

ABSTRACT: The primary barrier that protects our lungs against infection by pathogens is a tightly sealed layer of epithelial cells. When the integrity of this barrier is disrupted as a consequence of chronic pulmonary diseases or viral insults, bacterial pathogens will gain access to underlying tissues. A major pathogen that can take advantage of such conditions is *Staphylococcus aureus*, thereby causing severe pneumonia. In this study, we investigated how *S. aureus* responds to different conditions of the human epithelium, especially nonpolarization and fibrogenesis during regeneration using an *in vitro* infection model. The infective process was monitored by quantification of the epithelial cell and bacterial populations, fluorescence microscopy, and mass spectrometry. The results uncover differences in bacterial internalization and population dynamics that correlate with the outcome of infection. Protein profiling reveals that, irrespective of the polarization state of the epithelial cells, the invading bacteria mount similar responses to adapt to the intracellular milieu. Remarkably, a bacterial adaptation that was associated with the regeneration state of the epithelial cells concerned the early upregulation of proteins controlled by the redox-responsive regulator Rex when bacteria were confronted with a polarized cell layer. This is indicative of the modulation of the bacterial cytoplasmic redox state to maintain homeostasis early during infection even before internalization. Our present observations provide a deeper insight into how *S. aureus* can take advantage of a breached epithelial barrier and show that infected epithelial cells have limited ability to respond adequately to staphylococcal insults.

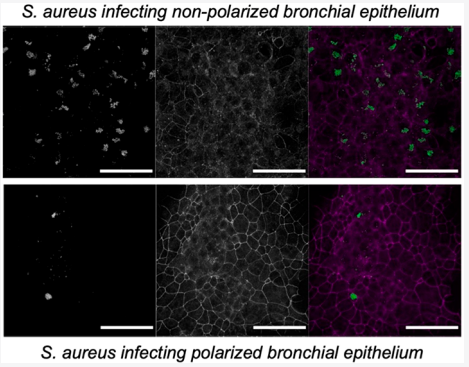

KEYWORDS: *infectious disease, host−pathogen interaction, Staphylococcus, energy, metabolism, virulence*

Staphylococcus aureus is an opportunistic pathogen[1] that is renowned for its ability to colonize several sites in the human body.[2,3] One of the most frequent sites of colonization is the upper respiratory tract, where it is commonly found as a commensal bacterium residing in the nose and throat.[4,5] However, *S. aureus* also has the potential to infect the lower parts of the respiratory tract, causing severe infections, including necrotizing pneumonia.[6,7] Although these infections can occur in community or hospital settings, the development of a chronic lung infection is commonly associated with pre-existing infections by other agents or with lung-associated diseases, like chronic obstructive pulmonary disease (COPD), cystic fibrosis (CF), or bronchiectasis.[8−14]

The epithelial cell layer of the lungs is our first barrier of defense against airborne pathogenic bacteria. Nevertheless, in the aforementioned conditions, the outermost layer of the lungs gets damaged, leading to wounded patches in the epithelium. After damage, the epithelial cell layer will pass through a process of healing that starts with the migration of epithelial cells to repopulate the created gap, followed by activation of the polarization machinery and fibrogenesis.[15−17] The latter involves regulatory pathways like sonic hedgehog signaling (Shh), transforming growth factor beta (TGFB), and Wingless/Integrated (Wnt) pathways, which are commonly deregulated in chronic lung diseases and could lead to permanent fibrosis.[18−20] These pathological conditions affect several functions of the epithelium, including correct localization of proteins in the cellular membrane, homogeneity of the epithelial layer, transport gradients, direction of cell division, and the permeability.[21,22] Consequently, the affected sites are regarded as portals for invasion of underlying tissues by *S. aureus* or other pathogens.[15,22]

To date, most studies on the mechanisms employed by *S. aureus* to breach epithelial barriers focused on model systems that mimic one particular state of the epithelial cells. On this basis, it is known that *S. aureus* weakens the epithelial layer by secreting toxins that disrupt the polarized cells, enabling the pathogen to cross the barrier and enter host cells.[23,24] Upon entry, the bacteria adapt to the intracellular milieu where they

Received: June 10, 2020
Published: June 24, 2020

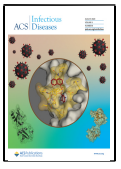

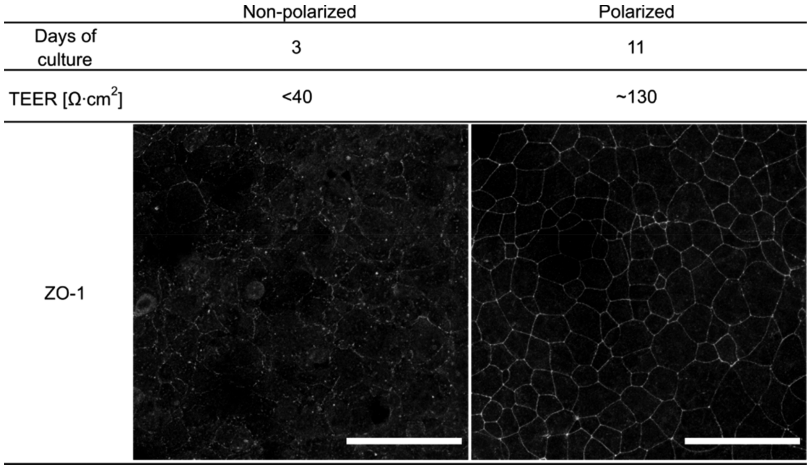

Figure 1. Epithelial cell layers with distinctive polarization states. The cell line 16HBE14o- was cultured for 3 and 11 days in order to obtain confluent cell layers with two different polarization states. The polarization states were monitored by measurements of the TEER and by immunostaining with an antibody specific for Zonula-Occludens 1. The micrographs present the maximum pixel value of the *Z*-stacks of the epithelial cell layers. Scale bar: 100 μm.

have to face nutrient scarcity and defensive host mechanisms. To do so, the bacteria activate pathways related to energy generation from the most readily available sources and balance the expression of virulence factors to take optimal advantage of their host.[25−28] However, an important knowledge gap relates to the question how *S. aureus* responds to different states of the human epithelium, such as nonpolarization or fibrogenesis during regeneration. Therefore, the aim of this study was to define possible differential responses of *S. aureus* to such preinfection conditions with a focus on changes at the proteome level. To this end, we devised an *in vitro* model that simulates staphylococcal infection at two different stages of epithelial regeneration. The first stage involves a layer of nonpolarized cells, which mimics the earliest stage of regeneration where the bacteria have "easy access" to the epithelium. The second involves a polarized host cell layer at the stage of fibrogenesis, where the bacteria can only gain access to the cells by disruption of the tight junctions connecting the regenerating epithelial cells. The results obtained with this model reveal distinct bacterial internalization rates depending on the stage of epithelial regeneration. While the bacteria displayed similar adaptations at the proteome level during the course of infection, the timing of these adaptations differed. Remarkably, differences are most clearly evident for proteins under control of the redox regulator Rex, where induction of Rex-regulated proteins is observed at an earlier time point when the bacteria are confronting polarized epithelial cells. Our observations indicate that bacteria approaching the polarized epithelial barrier encounter redox stress conditions that prompt earlier adaptations and likely influence the internalization process in nonprofessional phagocytic cells.

RESULTS

Distinctive Protein Abundances Define Regenerative Stages of Bronchial Epithelial Cells. The epithelial cell line 16HBE14o- is known for its capacity to form tight junctions, polarize, and differentiate,[29,30] which makes it suitable for the development of cell layers with regenerating phenotypes. To obtain two cell layers with distinctive characteristics, the cells were cultured over a porous Transwell support under the same conditions for different time periods. The first distinctive characteristic between the cell layers after 3 or 11 days of culturing was their polarization state (Figure 1), which was shown by the measurement of trans-epithelial electrical resistance (TEER) and immunofluorescence of the tight junction protein Zonula Occludens-1 (ZO-1). A layer of 16HBE14o- cells reaches its highest resistance after 14 days of culture (Figure S1). Therefore, to represent different regenerative states, the cell layer should display different polarization at the time points analyzed and, accordingly, we decided to culture the cells for 3 and 11 days. Importantly, the epithelial cell layer cultured for 3 days reached a state of confluency, but it did not develop polarity as evidenced by a marginal increase in resistance and the absence of ZO-1 localization at the lateral sites of the cell membranes. In contrast, the cell layers cultured over 11 days displayed an at least 3-fold increased electrical resistance consistent with a more organized localization of ZO-1 (Figure 1).

To further characterize the 16HBE14o- cells at different stages of polarization, their cytosolic proteome was profiled by data-independent acquisition (DIA) mass spectrometry (MS). In total, the levels of 3498 proteins were quantified. Of these, 1633 proteins presented significantly (p-value < 0.01) different levels at the two investigated time points (Table S1; column "p-value comparison"). More than half of the latter proteins were related to the production of the extracellular matrix (ECM) as well as pathways related to healing, like TGFB, Shh, and Wnt (Figure 2). Of note, several proteins of the core matrisome (i.e., the ensemble of all ECM proteins and ECM-associated proteins) were detected at differing levels, despite the fact that most of them are secreted during ECM production (Figure 2B). Considering the distinct protein abundance signatures that were observed, we conclude that the cells represent distinctive regenerative stages after 3 or 11 days of culturing, respectively.

Rate of *S. aureus* Internalization Differs at the Two Polarization States of the Host Cell Layer. After 3 or 11 days of culturing, the developed epithelial cell layers were infected with *S. aureus* for 1 h. Subsequently, the medium was replaced; noninternalized bacteria were killed by the addition of lysostaphin, and the course of infection was followed by immunofluorescence confocal microscopy (Figure 3A; Figures

https://dx.doi.org/10.1021/acsinfecdis.0c00403
ACS Infect. Dis. 2020, 6, 2279−2290

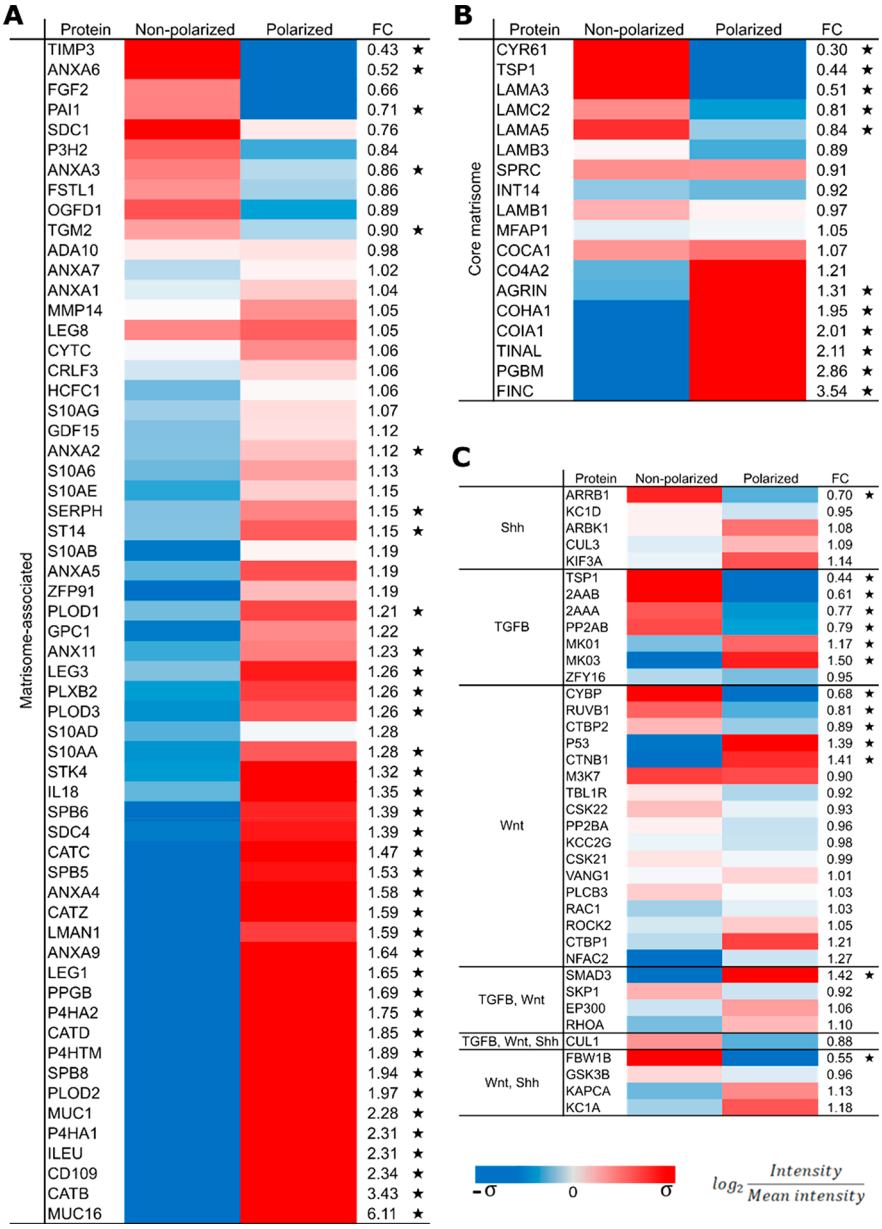

Figure 2. The epithelial cell layer models represent two different stages of wound regeneration. The nonpolarized layer was obtained after 3 days of culturing and the polarized layer, after 11 days of culturing. (A, B) Levels of matrisome-associated proteins and proteins of the core matrisome. (C) Levels of proteins related to major signaling pathways involved in tissue regeneration after injury. The indicated levels of expression are ratios of the levels at 0 h to the mean value quantification for the respective protein in both conditions at every time point of the experiment. The fold change (FC) measured for each individual protein is included in the column FC. Significant differences (p-value < 0.01) are marked with a star. $\sigma = 0.26$; Shh, sonic hedgehog signaling pathway; TGFB, transforming growth factor beta signaling pathway; Wnt, Wingless/Integrated pathway.

S2, S3, and S4) and quantification by flow cytometry of both the host and bacterial populations (Figure 3B–D). Imaging of the infection at 2.5 h post-infection (p.i.) showed that the bacterial internalization in cells of a nonpolarized cell layer is highly effective and that the bacterial clusters distributed homogeneously within the cell layer. In contrast, the infection of cells in a polarized cell layer occurred at specific sites of the cell layer where disruption of the tight junctions is evident (Figure S5).

Also, the progression of infection was different at the two different polarization states of the cultured cells. In non-polarized cells, the *S. aureus* population increased during the first 24 h of infection. Death of a considerable percentage of the host cell population became clearly evident from 24 h p.i. onward (Figure 3B), when the bacterial numbers had doubled (Figure 3C). At 48 h p.i., the integrity of the host cell layer was severely disrupted as evidenced by a decrease of the TEER (Figure 3D). The bacteria internalized by polarized cells also multiplied during the first hours of infection, which coincided with a slight decrease in the TEER at 24 h p.i. However, in this case, the epithelial cell layer did not display apparent damage or drastic changes in total cell numbers. On the other hand, the host cell population harboring bacteria at 48 h p.i. represented merely 3% of the total cell count.

Bacterial Proteome Profiles Mirror Adaptations to Epithelial Cell Layer Integrity. Quantitative proteome profiling (DIA-MS) was applied to visualize the adaptations of host cells and infecting bacteria during the first 6.5 h p.i.

https://dx.doi.org/10.1021/acsinfecdis.0c00403
ACS Infect. Dis. 2020, 6, 2279−2290

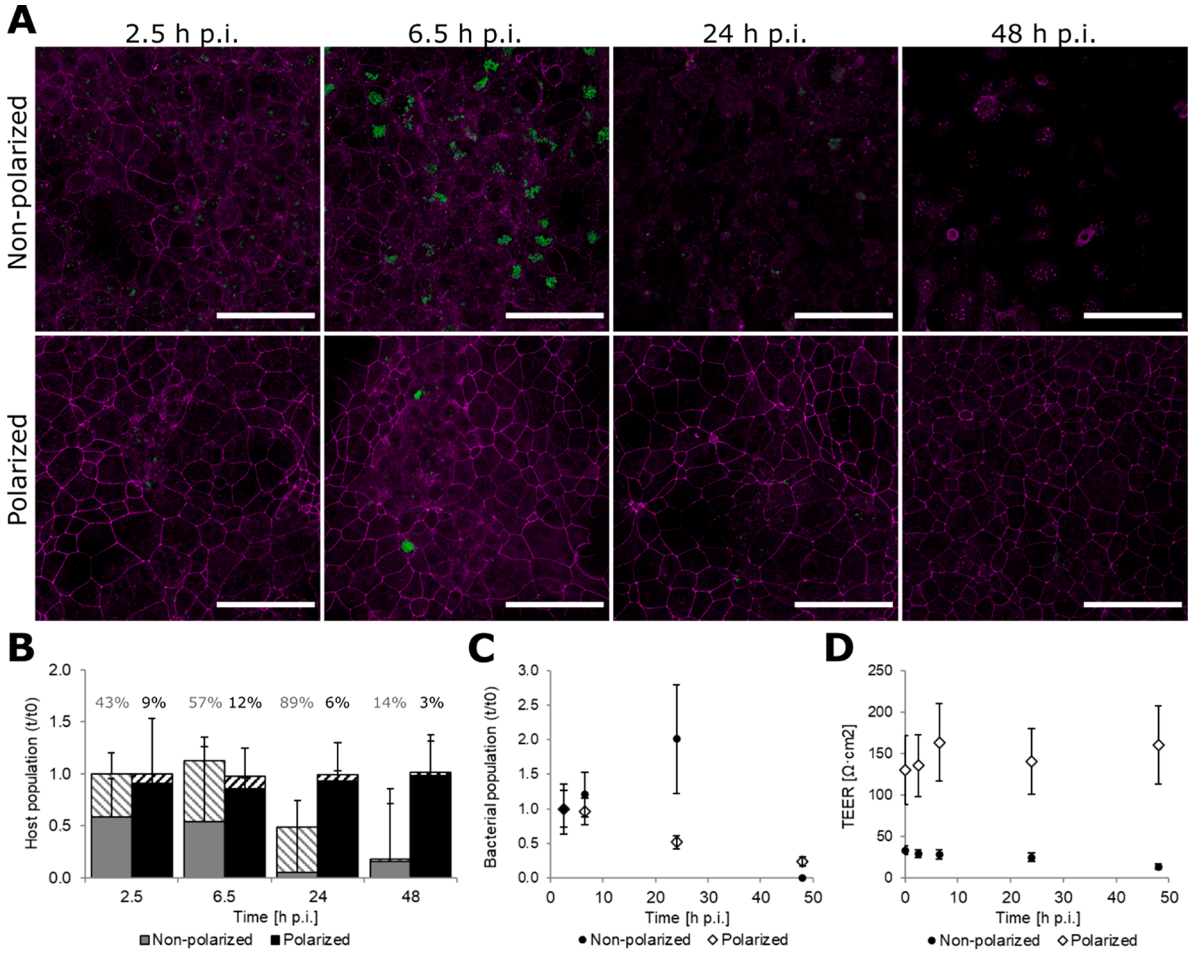

Figure 3. Dynamics of bacterial and host populations p.i. (A) Development of the *S. aureus* infection and integrity of the cell layer were tracked by immunofluorescence microscopy. The presented micrographs are the maximum pixel values of the *Z*-stacks of the infected cell layers. ZO-1 is depicted in magenta and *S. aureus*, in green. The individual representations of each channel are shown in Figures S2 and S3. Quantification of the bacterial fluorescence is shown in Figure S4. Scale bar: 100 μm. (B, C) Counting of the host and bacterial cell populations by flow cytometry. The changes over time are displayed in relation to 0 h p.i. (t/t_0). The proportion of epithelial cells that contain intracellular *S. aureus* at each time point is represented in panel B by the complemented bars marked with stripes; the respective percentages are indicated above each bar. (D) The polarity of the cell layer was tracked during infection by TEER measurements. All results of panels B–D are the average of 4 independent biological replicates.

Although the epithelial cell layers differed drastically in the initial protein abundances as mentioned above, no major changes in host cell protein dynamics were detectable upon infection with *S. aureus* (Table S1). In contrast, the bacterial proteome was highly dynamic; of the 1108 proteins monitored, more than 50% presented significant changes during the first 6.5 h p.i. (p-value < 0.05; Table S2). Interestingly, most of these proteins displayed a similar behavior in both settings of infection indicating that, by and large, the bacteria went through similar adaptive processes. However, the timing of the adaptive changes was markedly different for 67 staphylococcal proteins, depending on the stage of regeneration of the infected epithelial cell layer (Figure S6).

In order to appreciate the differences in *S. aureus* adaptation to epithelial cells at different stages of regeneration, the proteins displaying changes in level prior and during internalization were grouped according to their known regulators as described by Nagel et al.[31] Proteins in which the level is subject to the control by CodY, Agr, Sae, Fur, Rex, and SigB displayed infection-related changes in level (Figure 4). However, most clusters of proteins controlled by particular regulators did not show a differential behavior that could be associated with a specific host cell regeneration state. This was different for proteins controlled by the redox regulator Rex, where ∼50% of these proteins displayed differential behavior (Figure 4), namely, an earlier increase in level when the bacteria were confronted with polarized host cells. This difference in regulation also became clearly evident in a clustering of identified proteins based on metabolic pathways, where proteins related to fermentation were found to be upregulated at earlier time points (Figure 5A). On the contrary, such a different time dependency in regulation between *S. aureus* challenged by polarized vs nonpolarized host cells was not observed for other pathways related to energy acquisition, like the TCA cycle and oxidative phosphorylation, and for the majority of proteins involved in oxidative stress management (Figure 5A,B).

DISCUSSION

The epithelial cell layer in the human lung forms an important primary barrier against infection. Breaches of this barrier are dangerous as they provide easy access to pathogens that can

https://dx.doi.org/10.1021/acsinfecdis.0c00403
ACS Infect. Dis. 2020, 6, 2279−2290

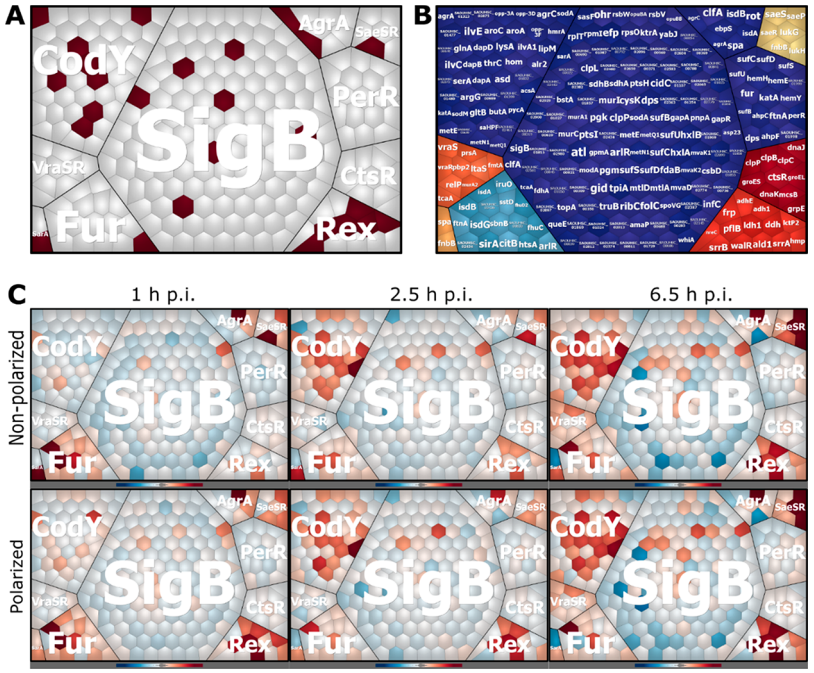

Figure 4. Voronoi tree map representation of *S. aureus* protein levels grouped by major regulators. (A) Proteins that displayed significantly (p-value < 0.05) different dynamics during the first 6.5 h p.i. between the two infection models are highlighted in maroon. (B) Names of the proteins represented in each polygon of the other panels. (C) Changes in protein amounts are presented at every time point relative to the respective protein quantities in the exponential phase. Increased levels are presented in dark red and decreased levels, in blue. The 1 h sample represents the fraction of bacteria in the medium that was neither internalized into nor attached to the host cells after addition of the bacterial master mix.

then not only invade underlying tissues but also cause additional damage to the epithelium by entering the respective cells from the basolateral side. Ultimately, this may lead to pneumonia, severe damage of the lungs and, in the worst case, death of the patient. Consequently, effective repair of a damaged lung epithelium is believed to be critical to avoid potentially life-threatening pulmonary infections. Despite this, it has so far not been studied in detail how different stages of regeneration of the epithelial layer determine the outcome of a bacterial infection and how these stages are reflected in the adaptive responses that take place in infecting bacteria. In the present study, we sought to improve our understanding of these interactions by establishing an infection model where epithelial cell layers were exposed to *S. aureus* at two distinct early stages of regeneration. In this respect, it should be noted that, upon lung injury, the epithelial cells will go through different stages of recovery that include inflammation and fibrogenesis phenotypes.[15,22] As shown by Schiller et al.,[17] protein expression post-injury is highly dynamic, and particular proteins play different roles in recovery over time. These regenerative stages were reflected in the proteins we identified in lung epithelial cells cultured for 3 or 11 days in our experimental setup. In particular, the high levels of the SERPINH1, ST14, PLOD1, LGALS3, PLXB2, PLOD3, CTSZ, LGALS1, CTSA, P4HA2, CTSD, PLOD2, TINAGL1, P4HA1, CTSB, and FN1 proteins as detected in polarized 16HBE14o- cells can be regarded as a proteomic signature for fibrogenesis.[17] Likewise, the detected low abundance of the TIMP3, THBS1, LAMA3, FGF2, LAMA5, and LAMB3 proteins is also a clear indicator for fibrinogenesis during polarization.[17] On this basis, the nonpolarized epithelial cell layer obtained after 3 days of culturing seems to resemble the initial migratory state of a damaged lung epithelium. In contrast, the polarized epithelial cell layer obtained after 11 days of culturing serves as a model for a subsequent early stage of fibrogenesis.

The dynamics of *S. aureus* infection in the two model stages of lung epithelial regeneration reflect the *in vivo* course of an infection remarkably well. As documented by microscopy, the infecting staphylococci had a clear impact on the epithelial cells during the first 6.5 h p.i., where the bacteria first disrupted the polarized cell layer and subsequently started to replicate intracellularly in both polarized and nonpolarized cells. Of note, bacterial replication was substantially stronger in the nonpolarized cells. Unexpectedly, this difference had no distinctive effect on the epithelial cells' proteome. Of course, in the case of the polarized cells, the rate of bacterial internalization is relatively low, so it is intuitive that changes in the host's proteome may have passed unnoticed. On the contrary, one might expect more severe changes in the proteome of nonpolarized epithelial cells that are virtually defenseless to the invading staphylococci. In particular, only two and nine proteins showed significantly different changes in the polarized and nonpolarized epithelial setups, respectively, after challenge with *S. aureus* (Table S1). Presumably, changes in the epithelial cell proteome will be more severe during later time points p.i. when the infection will probably elicit severe apoptotic reactions, but this can unfortunately not be assessed in our present experimental setup. However, the latter view seems realistic based on the findings from our previous study, where the effects of staphylococcal internalization on submerged 16HBE14o- lung epithelial cells were studied over a period of 96 h.[27]

The differential rates of *S. aureus* internalization by polarized and nonpolarized epithelial cells probably reflect the fact that fibronectin, one of the major host cell anchors for *S. aureus*, is exposed exclusively at the basolateral side of polarized epithelial cells.[32,33] The fact that this protein is essentially

https://dx.doi.org/10.1021/acsinfecdis.0c00403
ACS Infect. Dis. 2020, 6, 2279−2290

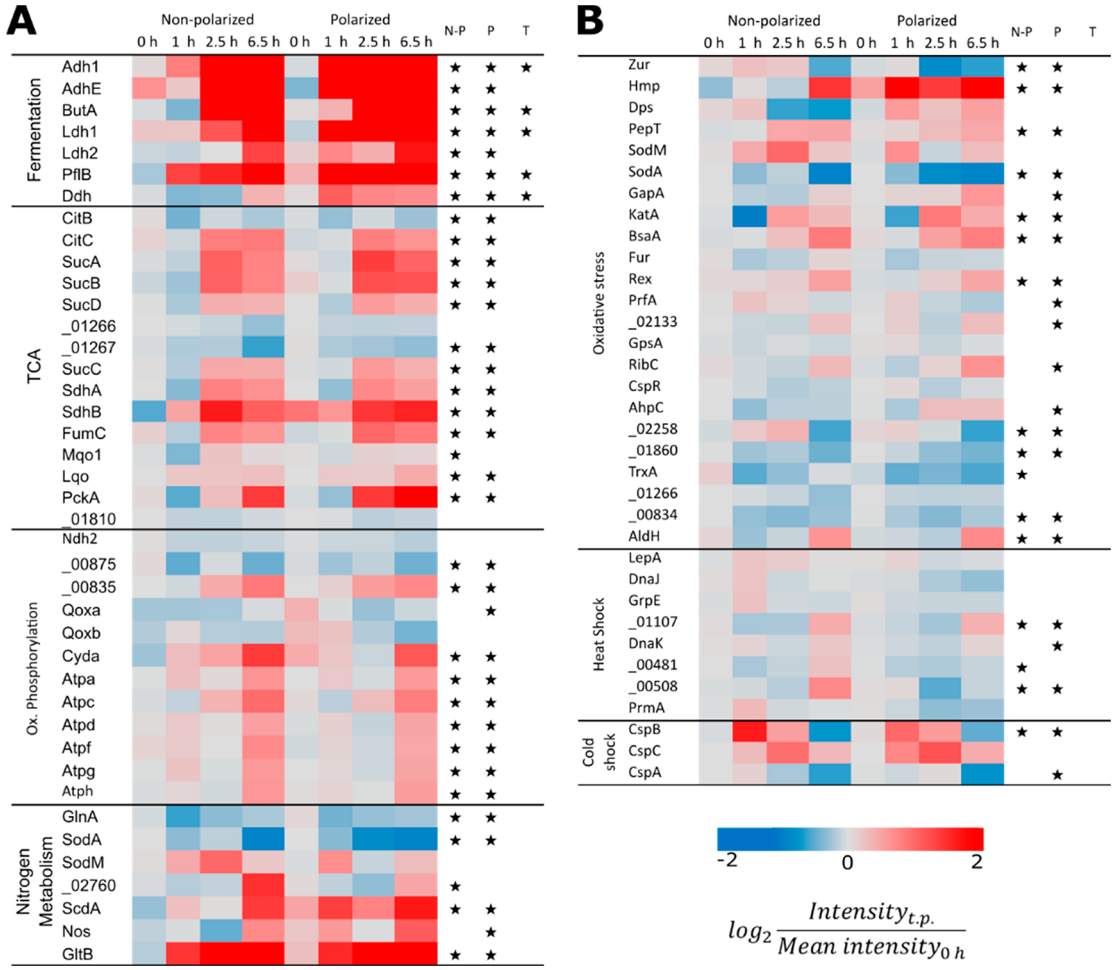

Figure 5. Central carbon and nitrogen metabolism of *S. aureus* during infection-related stress conditions. The levels of a selection of proteins related to (A) carbon and nitrogen metabolism and (B) stress conditions are represented in relation to the mean values measured for proteins extracted from the bacteria in the exponential growth phase at OD_{600} = 0.4. Significant changes (p-value < 0.05) are marked with stars in the last three columns, which relate to changes over time during nonpolarized conditions (N−P), polarized conditions (P), and the comparison of both trends (T). *S. aureus* proteins without an assigned gene symbol are labeled according to their locus tag without the "SAOUHSC_" identifier.

absent from the apical cell surface severely restricts the bacterial internalization.[34] *S. aureus* overcomes this challenge by the disruption of tight junctions between the epithelial cells with the aid of the pore-forming toxin Hla.[23,35−37] Although the production of Hla was not detectable in the cytosolic proteome fraction of the investigated bacteria, its presence can be inferred from the observed regulation of other proteins that are also controlled by the Agr quorum sensing system, such as ClfA and Spa.[36]

While the polarized epithelial cell layer is capable of overcoming the imposed staphylococcal infection, the infected nonpolarized epithelium is heading for disaster. In particular, strongly replicating internalized bacteria will almost inevitably induce massive cell death during the first day of infection.[26,27] Bacteria thus liberated from the epithelial enclosure will be released into the external milieu where, in principle, they can engage in another round of host cell infection. However, under our present experimental conditions, the latter will not be observed as the released bacteria are eliminated by lysostaphin that was added to the culture medium at 1 h p.i. Interestingly, when nonpolarized epithelial cells were challenged with *S. aureus*, the percentage of infected cells increased over time as a result of dying noninfected cells. Possibly, this is a consequence of the release of epithelial or bacterial debris into the medium that can induce apoptosis.

Despite the observed differences in infection dynamics, the adaptations of *S. aureus* p.i. were largely similar in polarized and nonpolarized epithelial cells, showing that the main bacterial adaptations to the infection conditions do not depend on the polarization state of the host cells. Such adaptations include elevated production of proteins related to the catabolism of alternative carbon sources, the degradation of amino acids, and the TCA cycle. Moreover, also the levels of proteins regulated by SaeRS and Agr, which have been linked to virulence, changed upon internalization (Table S2). Remarkably, we observed no differences in the dynamics of bacterial proteins responsive to oxidative-, heat-, or cold-stress conditions between the two infection settings.

The earlier upregulation of Rex-regulated proteins in bacteria facing a polarized epithelial barrier is indicative of a critical difference in the local conditions with potential implications for the internalization process and the course of infection. The Rex regulon is known to respond to changes in the NAD^+/NADH ratio of the bacterial cytoplasm, which may relate to limited availability of oxygen, excessive TCA cycle activity and rapidly increasing NADH concentration, or increased levels of NO.[38,39] As a consequence, the bacteria

https://dx.doi.org/10.1021/acsinfecdis.0c00403
ACS Infect. Dis. 2020, 6, 2279−2290

will upregulate pathways for anaerobic metabolism. This behavior could have been anticipated on the basis of the fact that NO is a signaling molecule employed in wound repair[40] and, therefore, produced in higher quantities during illnesses that compromise the lung epithelium like asthma and COPD.[41−44] In addition, NO production is a known anti-infective defense mechanism employed by human host cells.[45−47] Accordingly, the differential timing in the detection of Rex-regulated proteins is potentially a consequence of redox stress conditions at 1 h p.i. Of note, once internalized, the fermentative pathways will be further upregulated as a consequence of the microaerobic environment that the bacteria are exposed to intracellularly.[26−28]

Lastly, a limitation of our present experimental setup is that it is currently still very difficult to validate the obtained proteomics data by independent experiments, especially where it concerns the proteome dynamics of the intracellular bacteria. The absolute numbers of internalized bacteria are low, which makes validation of the data by quantitative Western blotting or protein activity assays challenging. This is further complicated by a general lack of specific antibodies and the fact that it is hard to distinguish many of the metabolic enzyme activities of internalized bacteria from those of the host cells. An alternative option would be to validate the observed effects by transcriptome analyses, which would require sorting of larger numbers of bacteria that would be difficult to accomplish particularly at late time points. On the other hand, we would like to point out that the data presented for particular Rex-regulated proteins or proteins involved in bacterial metabolism validate each other. Even though the quantifications were independently performed for each protein, the data are connected in the form of proteomic signatures that show consistent regulatory effects at the regulon level and for metabolic pathways.

■ CONCLUSION

Here, we explored the adaptive behavior of *S. aureus* upon close encounters with polarized and nonpolarized lung epithelial cells that mimic the clinical situation of a wounded epithelium at different early regenerative stages. In the clinical context, such scenarios will be encountered, in particular, when the lung epithelial cell layer is damaged by common pathogens, such as influenza.[12,48] Our present observations provide a deeper insight into how the *S. aureus* bacterium may take advantage of such a breach of barrier and how infected epithelial cells have a limited ability of responding to the staphylococcal insult, especially during the very early stages of tissue regeneration. Our study also highlights early adaptations of *S. aureus*, where the upregulation of proteins under the control of Rex could be critical for the confrontation with polarized epithelial cells to maintain bacterial homeostasis and to stay fit for infection.

■ METHODS

Bacterial Strains and Culture Conditions. *S. aureus* strain HG001[49] carrying plasmid pJL76 with a codon optimized GFP[50] was used for internalization experiments into epithelial cells followed by mass spectrometry (MS) analyses. For immunofluorescence microscopy, a Δ*spa* mutant was used to avoid unspecific binding of the antibodies.

Cultivation of bacteria was carried out in prokaryotic minimal essential medium (pMEM): 1× MEM without sodium bicarbonate (Invitrogen, Karlsruhe, Germany) supplemented with 1× nonessential amino acids (PAN-Biotech GmbH, Aidenbach, Germany), 4 mM L-glutamine (PAN-Biotech GmbH, Germany), 10 mM HEPES (PAN-Biotech GmbH), 2 mM L-alanine, 2 mM L-leucine, 2 mM L-isoleucine, 2 mM L-valine, 2 mM L-aspartate, 2 mM L-glutamate, 2 mM L-serine, 2 mM L-threonine, 2 mM L-cysteine, 2 mM L-proline, 2 mM L-histidine, 2 mM L-phenyl alanine, and 2 mM L-tryptophan (all from Sigma-Aldrich, Schnelldorf, Germany), adjusted to pH 7.4 and sterilized through filtration.

The cultivation of the samples was performed as described previously.[51] In brief, overnight cultures were done as serial dilutions in media enriched with 0.01% yeast extract. Additionally, all overnight cultures contained 10 μg/mL erythromycin (Sigma-Aldrich) to maintain pJL76, and 10 μg/mL tetracycline (Sigma-Aldrich) was added to cultures of the Δ*spa* mutant. Cultures were incubated for 16 h in an orbital shaking incubator at 37 °C and 220 rpm. All main cultures for infection experiments were prepared in pMEM without yeast extract or antibiotics and inoculated with a bacterial master mix prepared from overnight cultures in the midexponential phase. Incubation of the main cultures was carried out in a shaking water bath at 37 °C and 150 rpm.

Cell Lines and Culture Conditions. The immortalized 16HBE14o- epithelial cell line is derived from transformed bronchial epithelial cells of a 1-year-old heart−lung transplant patient.[29] Cultivation of the cells was carried out in eukaryotic minimal essential medium (eMEM): 1× MEM with Earle's salts with 2.2 g/L $NaHCO_3$ (Biochrom AG, Berlin, Germany) supplemented with 10% (v/v) fetal calf serum (FCS; Biochrom AG), 2% (v/v) L-glutamine (200 mM, PAN-Biotech GmbH), and 1% (v/v) nonessential amino acids (100×, PAN-Biotech GmbH). The cells were cultured in 10 cm plates at 37 °C and 5% CO_2 in a humid atmosphere and were kept for no more than 15 passages.

The seeding of the cells was done at a density of 1×10^5 cells/cm^2 over a 12 mm Transwell polyester membrane with 0.4 μm pore size (Corning, Schnelldorf, Germany) to promote the polarization of the cell layer. Cells were cultured for 3 or 11 days, depending on the desired condition for infection. The volume of medium on the apical side was 400 μL, and it was 1300 μL on the basal side. The medium was exchanged every second day until day eight after which the exchange was done daily.

Measurement of Transepithelial Electrical Resistance. Bioelectric measurements were performed with an EVOMX Volt-ohmmeter equipped with STX2 chopstick electrodes (WPI, Berlin, Germany). To measure the resistance of the cell layer, the medium of every cultured Transwell was replaced with prewarmed eMEM medium (500 and 1500 μL on the apical and basal sides, respectively) and equilibrated for 10 min at room temperature. The TEER was calculated by subtracting the blank measurement and subsequently multiplying it by the area of the Transwell. After measurement, the medium was exchanged with prewarmed fresh medium.

Internalization Procedure. The protocol for infection was based on the methods described by Pförtner et al.[51] with some adaptations for infection in Transwells. The bacterial main cultures were inoculated at a starting OD_{600} of 0.05, grown until midexponential phase, and collected at an OD_{600} of ∼0.4. Prior to infection, the number of bacterial cells was determined by flow cytometry with a Guava easyCyte flow cytometer (Merck Millipore, Darmstadt, Germany), using a

https://dx.doi.org/10.1021/acsinfecdis.0c00403
ACS Infect. Dis. 2020, 6, 2279−2290

blue 50 mW laser to excite bacterial GFP that allowed quantification of the bacteria. The same day of infection, epithelial cells were counted after detachment from the porous membrane by 5 min of incubation at 37 °C with 0.25% trypsin-EDTA (Gibco, Grand Island, NY). Then, the cell solution was mixed in equal quantities with trypan blue dye, and the cell number was quantified with a Countess (Invitrogen).

Infection of host epithelial cells with *S. aureus* was carried out by exchange of the apical medium with the infection mix. This solution contained *S. aureus* diluted in eMEM to a multiplicity of infection of 25 and buffered with 2.9 μL of sodium hydrogen carbonate (7.5%, PAN-Biotech GmbH) per mL of bacterial culture. Epithelial cells were exposed to the bacteria for 1 h at 37 °C and 5% CO_2. Afterward, the media on the apical and basal sides were exchanged with fresh eMEM medium containing 10 μg/mL lysostaphin (AMBI Products LLC, Lawrence, NY).

Sampling for counting of 16HBE14o- cells at every time point was performed as described above and, additionally, the number of infected cells was counted in the Guava easyCyte flow cytometer. The collection of internalized bacteria was done by incubation with 0.05% sodium dodecyl sulfate (SDS; Carl Roth, Karlsruhe, Germany) for 5 min at 37 °C, and quantification of bacteria was performed using a Guava easyCyte.

Immunofluorescence Staining. 16HBE14o- cells were cultured over Transwell supports for 3 or 11 days. The medium of the wells was removed, and the cells were washed with phosphate-buffered saline (PBS). Fixation of cells was done with 5% acetic acid in absolute ethanol for 10 min at room temperature. To avoid autofluorescence, the supports were incubated for 15 min at room temperature with 50 mM NH_4Cl. Subsequently, permeabilization of the cells and blocking of nonspecific binding were carried out. To this end, cells were incubated for 30 min at room temperature with 0.2% bovine serum albumin (BSA) and 0.1% saponin in PBS, followed by overnight incubation at 4 °C with 2% BSA, 0.1% saponin, and 5% Neutral Goat Serum in PBS. Additional blocking was performed with 12 μg/mL of a human monoclonal antibody (1D9[52]) diluted in the same blocking solution for 2 h at room temperature in a humidifier chamber. Thereafter, immunofluorescence staining was carried out using a rabbit polyclonal antibody against ZO-1 (40-2200; Invitrogen) in a 1:100 dilution and a goat polyclonal secondary antibody against rabbit conjugated with alexa fluor 647 (A-21244; Thermo Fisher Scientific, Landsmeer, The Netherlands) in a 1:2000 dilution. The incubation of antibodies was done separately, each for 1 h at room temperature in a humidifier chamber. The cells were washed with blocking solution between incubations. Finally, the DNA was stained with 4′,6-diamidino-2-phenylindole (DAPI) by incubation for 15 min at room temperature, and the slides were mounted with Mowiol 4-88 (EMD 208 Chemical, Inc., Temecula, CA). Visualization of the samples was done using a Leica SP8 microscope at the UMCG Microscopy and Imaging Center.

Sample Preparation for Mass Spectrometry. The sample preparation of human lung epithelial and bacterial samples was performed as described before in detail.[26,27]

Briefly, the collection of epithelial cell samples was carried out at the beginning of the infection and 1, 2.5, and 6.5 h p.i. by disruption with UT buffer (8 M urea, 2 M thiourea in MS-grade water, Sigma-Aldrich) and immediate freezing in liquid nitrogen. Further disruption of the cells was done by 5 cycles of freeze−thawing using liquid nitrogen and shaking at 30 °C, followed by ultrasonication with a Sonopuls homogenizer (Bandelin electronic, Berlin, Germany) in 3 cycles of 3 s at 50% power and 1 min of cooling on ice. The samples were centrifuged at maximal speed (~20 000*g*) for 1 h at 4 °C; the supernatant was collected, and the protein concentration of the samples was quantified using a Bradford assay (Biorad, Hercules, CA). Samples containing 4 μg of protein were prepared for MS by reduction with 2.5 mmol/L dithiothreitol (Thermo Fisher Scientific) for 1 h at 60 °C and alkylation with 10 mmol/L iodoacetamide for 30 min at 37 °C. Lastly, samples were digested with trypsin (1:25 trypsin/protein; Promega, Madison, WI) at 37 °C overnight and purified using C_{18} columns (Merck Millipore).

S. aureus HG001 sampling for MS involved one sample of the main culture in midexponential phase, collection of the nonadherent bacteria after 1 h of infection, and samples of internalized bacteria collected at 2.5 and 6.5 h p.i. The last two samples were obtained by disruption of the host cells with 0.05% SDS for 5 min at 37 °C. All samples were concentrated by centrifugation for 10 min at 10 000*g* and 4 °C; the supernatant was removed, and the pellet was diluted in 2 mL of PBS. Subsequently, 2 million bacteria were sorted for each time point by flow cytometry using a FACSAria IIIu cell sorter (Becton Dickinson Biosciences, Franklin Lakes, NJ). Excitation of GFP was done with a 488 nm laser, and the emission signal was detected in a 515−545 nm range. Afterward, the bacteria were collected on low protein binding filter membranes with a pore size of 0.22 μm (Merck Millipore). The bacterial cells were lysed on the filter by incubation with 7.4 μg/mL lysostaphin in 50 mM ammonium bicarbonate for 30 min at 37 °C. Finally, digestion of the liberated proteins was performed with 0.3 μg of trypsin at 37 °C overnight, and tryptic peptides were purified using C_{18} ZipTip columns (Merck Millipore, Germany).

All purified peptides were resuspended in a buffer containing 2% acetronitile and 0.1% acetic acid in MS-grade water. Indexed Retention Time (iRT) peptides (Biognosys AG, Schlieren, Switzerland) were added to all samples of epithelial cells and bacteria for peak detection, mass calibration, noise reduction, and signal quantification. Samples were spiked according to the manufacturer's instructions, adding one injection equivalent of iRT peptide mix per injected volume. Bacterial samples had a final volume of 12 μL, of which 10 μL was injected, while 16HBE14o- samples were resuspended in 20 μL, with an injection volume of 5 μL.

Mass Spectrometry Measurements and Analysis. Separation of tryptic peptides was accomplished with a Dionex Ultimate 3000 nano-LC system (Dionex/Thermo Fischer Scientific) using an Accucore 150-C18 analytical column (25 cm × 75 μm, 2.6 μm C18 particles, 150 Å pore size, Thermo Fischer Scientific). The elution of peptides was carried out at constant temperature (40 °C) with a flow rate of 300 nL/min and a 120 min linear gradient of acetronitrile (2% to 25%) in 0.1% acetic acid. MS/MS measurements were performed on a QExactive (Thermo Fischer Scientific) in data-independent acquisition mode (DIA) following the method described by Bruderer et al.[53] Table S3 details the instrumental setup and parameters used for the measurements. In general, 19 isolation windows with a 2 m/z overlap were set to cover a mass range of 400−1220 m/z with a resolution of 35.000 for MS and MS/MS and an AGC target of 5×10^6 for MS and 3×10^6 for MS/MS.

https://dx.doi.org/10.1021/acsinfecdis.0c00403
ACS Infect. Dis. 2020, 6, 2279−2290

Proteins were identified and quantified using Spectronaut V11.0.18108.11.30271 software (Biognosys AG) against MS databases generated from data-dependent acquisition (DDA) measurements of either *S. aureus*[31] or epithelial cells[27] under different culture conditions. The bacterial ion library was constructed on the basis of the fasta file from AureoWiki[54] with 2.852 *S. aureus* protein entries, from which the final target−decoy version was generated by adding all reverse entries to a total of 5.944 entries. The human epithelium peptide library was constructed on the basis of DDA measurements from 16HBE14o- and S9 cells searched against a target−decoy database with 40.640 entries and was built on the basis of 20.217 Uniprot entries (February 2018). Both databases include 102 cRAP common contaminants (https://www.thegpm.org/crap/) and a concatenated iRT peptide entry. The peptide spectral matching was performed with a parent mass error of 30 and 20 ppm for bacterial and human libraries, respectively. Both searches allowed full-tryptic peptides (trypsin/P cleavage rule) with up to two missed internal cleavage sites, a fragment mass error of 0.01 Da, variable modification of +15.9949 for oxidized methionine, and fixed modification of +57.021464 for carbamidomethylated cysteine.

The settings for the Spectronaut analyses were a dynamic mass tolerance at MS1 and MS2, dynamic XIC retention time extraction window, automatic calibration, and dynamic decoy strategy (library size factor of 0.1, minimum limit of 5000). The search included fixed modifications of +57.021464 by carbamidomethylation of cysteine and variable modification of +15.9949 due to the oxidation of methionine. The *Q*-value cutoffs were set to 0.01 for proteins and 0.001 for precursors. Complete profiles with a *Q*-value < 0.001 were used to perform a local cross-run normalization, and the reported quantifications refer to the MS2 peak area. Missing ion values were parsed when at least 25% of all samples had high quality quantifications. The parsing was performed using iRT profiling with a carryover of exact peak boundaries (minimum *Q*-value row selection = 0.001) and only for precursors with a *Q*-value > 0.0001. To prevent false positives, the parsed values were filtered out if their values were more than 2-fold higher than the measured values. Table S4 summarizes all the settings used for the Spectronaut analyses.

Statistical Testing of Changes in Protein Abundances over Time. Further analysis considered only proteins with at least two peptides. Normalization of each peptide was performed on the basis of the mean value of all time points. The final protein dynamics was calculated as the median of all corresponding normalized peptides. A linear model was fitted for every protein using the LIMMA package version 3.34.9[55] in R version 3.4.4.[56] An empirical Bayes moderated *t* test was conducted for each protein to detect significant differences between polarized and nonpolarized cells. Moreover, every protein was tested individually in both conditions for changes over time by an empirical Bayes moderated F-test. All moderated *p*-values were corrected for multiple testing using Benjamini and Hochberg's multiple testing correction. Protein changes were assumed to be significant when their adjusted *p*-value was lower than 0.05 for the *S. aureus* proteome or lower than 0.01 for the epithelial cell proteome. The cutoff was more stringent for the host proteome due to the higher amount of proteins with different levels between the two epithelial conditions.

The annotation of identified proteins was based on the Uniprot database. For *S. aureus*, the annotation was complemented with the AureoWiki database[54] and the regulons as described by Nagel et al.[31] The latter was used as a database to draw Voronoi tree maps using the Paver 2.1 software (DECODON GmbH, Greifswald, Germany).

Experimental Design and Statistical Rationale. The MS measurements of host and pathogen were carried out on samples collected from four independent biological replicates of the infection experiments in both conditions of the epithelium. During these experiments, sample collection for quantification of both populations and TEER measurements were performed as well. This number of replicates ensured that every protein was measured consistently at least three times. For each experiment, 4 samples were collected over the first 6.5 h p.i. resulting in 16 samples of bacterial cytosolic proteome and 16 samples of intracellular host cell proteome per epithelial condition. Samples from bacteria and host were measured in two different batches and, to avoid consecutive measurements of samples of the same condition, the running order was randomized by assigning a number between 1 and 32 generated by function *sample* in R version 3.4.4.[56] Additionally, three independent infection experiments were performed for the collection of samples for imaging.

Two statistical tests were used to evaluate the differences between conditions: the Bayes moderated *t* test was applied to determine the differences in the protein levels between the two epithelial conditions, while the Bayes moderated F-test was used to determine changes in protein abundance over time. All moderated *p*-values were corrected for multiple testing using Benjamini and Hochberg's multiple testing correction.

Data and Software Availability. The raw files from the MS analyses have been deposited in *MassIVE* (https://massive.ucsd.edu) under MSV000083271 (16HBE14o-) and MSV000083269 (*S. aureus*). During the review process, these data can be accessed using the passwords "HBE_TW_palma" and "Saureus_TW_palma", respectively. After acceptance of the manuscript, the data will be made freely available. The raw output files from Spectronaut, including peptide ions and *Q*-values, are included in Tables S5 and S6. All protein annotations and median abundances are included in Tables S1 and S2.

■ ASSOCIATED CONTENT

Supporting Information

The Supporting Information is available free of charge at https://pubs.acs.org/doi/10.1021/acsinfecdis.0c00403.

Figure S1: Development of polarization in the epithelial cell layer measured by TEER; Figure S2: Immunofluorescence microscopy of nonpolarized epithelial cells infected with *S. aureus*; Figure S3: Immunofluorescence microscopy of polarized epithelial cells infected with *S. aureus*; Figure S4: Quantification of the intracellular bacterial population in polarized and nonpolarized cells; Figure S5: Immunofluorescence microscopy of polarized epithelial cells infected with *S. aureus* to illustrate colocalization of *S. aureus* infection with sections of the layer with a weakened tight junction; Figure S6: Heatmap of *S. aureus* proteins displaying different dynamics during infection; Table S3: Instrumental setup and parameters applied in the LC-MS/MS analysis for DIA measurement of proteins in the experimental samples (PDF)

https://dx.doi.org/10.1021/acsinfecdis.0c00403
ACS Infect. Dis. 2020, 6, 2279−2290

Table S1: Host proteins detected with at least 2 peptides (XLSX)
Table S2: *S. aureus* proteins detected with at least 2 peptides (XLSX)
Table S4: Settings, Spectronaut (XLSX)
Table S5: MS data HBE cells, raw Spectronaut (ZIP)
Table S6: MS data *S. aureus*, raw Spectronaut (ZIP)

AUTHOR INFORMATION

Corresponding Authors

Uwe Völker − *Interfaculty Institute for Genetics and Functional Genomics, University Medicine Greifswald, 17475 Greifswald, Germany*; Email: voelker@uni-greifswald.de

Jan Maarten van Dijl − *University of Groningen, University Medical Center Groningen, Department of Medical Microbiology, 9700 RB Groningen, The Netherlands*; orcid.org/0000-0002-5688-8438; Email: j.m.van.dijl01@umcg.nl

Authors

Laura M. Palma Medina − *Interfaculty Institute for Genetics and Functional Genomics, University Medicine Greifswald, 17475 Greifswald, Germany; University of Groningen, University Medical Center Groningen, Department of Medical Microbiology, 9700 RB Groningen, The Netherlands*

Ann-Kristin Becker − *Institute of Bioinformatics, University Medicine Greifswald, 17475 Greifswald, Germany*

Stephan Michalik − *Interfaculty Institute for Genetics and Functional Genomics, University Medicine Greifswald, 17475 Greifswald, Germany*

Kristin Surmann − *Interfaculty Institute for Genetics and Functional Genomics, University Medicine Greifswald, 17475 Greifswald, Germany*

Petra Hildebrandt − *Interfaculty Institute for Genetics and Functional Genomics, University Medicine Greifswald, 17475 Greifswald, Germany*

Manuela Gesell Salazar − *Interfaculty Institute for Genetics and Functional Genomics, University Medicine Greifswald, 17475 Greifswald, Germany*; orcid.org/0000-0002-6727-1978

Solomon A. Mekonnen − *Interfaculty Institute for Genetics and Functional Genomics, University Medicine Greifswald, 17475 Greifswald, Germany; University of Groningen, University Medical Center Groningen, Department of Medical Microbiology, 9700 RB Groningen, The Netherlands*

Lars Kaderali − *Institute of Bioinformatics, University Medicine Greifswald, 17475 Greifswald, Germany*

Complete contact information is available at: https://pubs.acs.org/10.1021/acsinfecdis.0c00403

Notes

The funders had no role in the study design, data collection and analysis, decision to publish, or preparation of the manuscript.
The authors declare no competing financial interest.

ACKNOWLEDGMENTS

We thank Jan Pané-Farré for providing *S. aureus* HG001 Δ*spa*. Funding for this project was received from the Graduate School of Medical Sciences of the University of Groningen [to L.M.P.M., S.A.M., and J.M.v.D.] and the Deutsche Forschungsgemeinschaft Grants GRK1870 [to L.M.P.M., S.A.M., and U.V.] and SFBTRR34 [to U.V.]. Part of this work has been performed at the UMCG Imaging and Microscopy Center (UMIC), which is sponsored by NWO grants 40-00506-98-9021 (TissueFaxs) and 175-010-2009-023 (Zeiss 2p).

REFERENCES

(1) Lowy, F. D. (1998) *Staphylococcus aureus* Infections. *N. Engl. J. Med. 339*, 520−532.
(2) Dastgheyb, S. S., and Otto, M. (2015) Staphylococcal adaptation to diverse physiologic niches: an overview of transcriptomic and phenotypic changes in different biological environments. *Future Microbiol. 10*, 1981−1995.
(3) Sollid, J. U. E., Furberg, A. S., Hanssen, A. M., and Johannessen, M. (2014) *Staphylococcus aureus*: Determinants of human carriage. *Infect., Genet. Evol. 21*, 531−541.
(4) Wertheim, H. F., Melles, D. C., Vos, M. C., van Leeuwen, W., van Belkum, A., Verbrugh, H. A., and Nouwen, J. L. (2005) The role of nasal carriage in *Staphylococcus aureus* infections. *Lancet Infect. Dis. 5*, 751−762.
(5) Krismer, B., Liebeke, M., Janek, D., Nega, M., Rautenberg, M., Hornig, G., Unger, C., Weidenmaier, C., Lalk, M., and Peschel, A. (2014) Nutrient Limitation Governs *Staphylococcus aureus* Metabolism and Niche Adaptation in the Human Nose. *PLoS Pathog. 10*, e1003862.
(6) Gillet, Y., Vanhems, P., Lina, G., Bes, M., Vandenesch, F., Floret, D., and Etienne, J. (2007) Factors Predicting Mortality in Necrotizing Community-Acquired Pneumonia Caused by *Staphylococcus aureus* Containing Panton-Valentine Leukocidin. *Clin. Infect. Dis. 45*, 315−321.
(7) Chen, J., Luo, Y., Zhang, S., Liang, Z., Wang, Y., Zhang, Y., Zhou, G., Jia, Y., Chen, L., and She, D. (2014) Community-acquired necrotizing pneumonia caused by methicillin-resistant *Staphylococcus aureus* producing Panton−Valentine leukocidin in a Chinese teenager: case report and literature review. *Int. J. Infect. Dis. 26*, 17−21.
(8) Zhang, Q., Illing, R., Hui, C. K., Downey, K., Carr, D., Stearn, M., Alshafi, K., Menzies-Gow, A., Zhong, N., and Fan Chung, K. (2012) Bacteria in sputum of stable severe asthma and increased airway wall thickness. *Respir. Res. 13*, 35.
(9) Pastacaldi, C., Lewis, P., and Howarth, P. (2011) Staphylococci and staphylococcal superantigens in asthma and rhinitis: a systematic review and meta-analysis. *Allergy 66*, 549−555.
(10) Papi, A., Bellettato, C. M., Braccioni, F., Romagnoli, M., Casolari, P., Caramori, G., Fabbri, L. M., and Johnston, S. L. (2006) Infections and Airway Inflammation in Chronic Obstructive Pulmonary Disease Severe Exacerbations. *Am. J. Respir. Crit. Care Med. 173*, 1114−1121.
(11) Wilkinson, T. M. A., Hurst, J. R., Perera, W. R., Wilks, M., Donaldson, G. C., and Wedzicha, J. A. (2006) Effect of Interactions Between Lower Airway Bacterial and Rhinoviral Infection in Exacerbations of COPD. *Chest 129*, 317−324.
(12) Chekabab, S. M., Silverman, R. J., Lafayette, S. L., Luo, Y., Rousseau, S., and Nguyen, D. (2015) *Staphylococcus aureus* Inhibits IL-8 Responses Induced by Pseudomonas aeruginosa in Airway Epithelial Cells. *PLoS One 10*, e0137753.
(13) Shah, P. L., Mawdsley, S., Nash, K., Cullinan, P., Cole, P. J., and Wilson, R. (1999) Determinants of chronic infection with *Staphylococcus aureus* in patients with bronchiectasis. *Eur. Respir. J. 14*, 1340−1344.
(14) Schwerdt, M., Neumann, C., Schwartbeck, B., Kampmeier, S., Herzog, S., Görlich, D., Dübbers, A., Große-Onnebrink, J., Kessler, C., Küster, P., Schültingkemper, H., Treffon, J., Peters, G., and Kahl, B. C. (2018) *Staphylococcus aureus* in the airways of cystic fibrosis patients - A retrospective long-term study. *Int. J. Med. Microbiol. 308*, 631−639.
(15) Puchelle, E., Zahm, J.-M., Tournier, J.-M., and Coraux, C. (2006) Airway epithelial repair, regeneration, and remodeling after injury in chronic obstructive pulmonary disease. *Proc. Am. Thorac. Soc. 3*, 726−733.

(16) Wilson, M., and Wynn, T. (2009) Pulmonary fibrosis: pathogenesis, etiology and regulation. *Mucosal Immunol. 2*, 103−121.
(17) Schiller, H. B., Fernandez, I. E., Burgstaller, G., Schaab, C., Scheltema, R. A., Schwarzmayr, T., Strom, T. M., Eickelberg, O., and Mann, M. (2015) Time- and compartment-resolved proteome profiling of the extracellular niche in lung injury and repair. *Mol. Syst. Biol. 11*, 819.
(18) Fernandez, I. E., and Eickelberg, O. (2012) New cellular and molecular mechanisms of lung injury and fibrosis in idiopathic pulmonary fibrosis. *Lancet 380*, 680−688.
(19) Kisseleva, T., and Brenner, D. A. (2008) Mechanisms of Fibrogenesis. *Exp. Biol. Med. 233*, 109−122.
(20) Kleinman, H. K., Philp, D., and Hoffman, M. P. (2003) Role of the extracellular matrix in morphogenesis. *Curr. Opin. Biotechnol. 14*, 526−532.
(21) Rodriguez-Boulan, E., and Macara, I. G. (2014) Organization and execution of the epithelial polarity programme. *Nat. Rev. Mol. Cell Biol. 15*, 225−242.
(22) Herard, A. L., Zahm, J. M., Pierrot, D., Hinnrasky, J., Fuchey, C., and Puchelle, E. (1996) Epithelial barrier integrity during *in vitro* wound repair of the airway epithelium. *Am. J. Respir. Cell Mol. Biol. 15*, 624−632.
(23) Räth, S., Ziesemer, S., Witte, A., Konkel, A., Müller, C., Hildebrandt, P., Völker, U., and Hildebrandt, J.-P. (2013) S. aureus haemolysin A-induced IL-8 and IL-6 release from human airway epithelial cells is mediated by activation of p38- and Erk-MAP kinases and additional, cell type-specific signalling mechanisms. *Cell. Microbiol. 15*, 1253−1265.
(24) Soong, G., Martin, F. J., Chun, J., Cohen, T. S., Ahn, D. S., and Prince, A. (2011) *Staphylococcus aureus* Protein A Mediates Invasion across Airway Epithelial Cells through Activation of RhoA GTPase Signaling and Proteolytic Activity. *J. Biol. Chem. 286*, 35891−35898.
(25) Kiedrowski, M. R., Paharik, A. E., Ackermann, L. W., Shelton, A. U., Singh, S. B., Starner, T. D., and Horswill, A. R. (2016) Development of an *in vitro* colonization model to investigate *Staphylococcus aureus* interactions with airway epithelia. *Cell. Microbiol. 18*, 720−732.
(26) Michalik, S., Depke, M., Murr, A., Gesell Salazar, M., Kusebauch, U., Sun, Z., Meyer, T. C., Surmann, K., Pförtner, H., Hildebrandt, P., Weiss, S., Palma Medina, L. M., Gutjahr, M., Hammer, E., Becher, D., Pribyl, T., Hammerschmidt, S., Deutsch, E. W., Bader, S. L., Hecker, M., Moritz, R. L., Mäder, U., Völker, U., and Schmidt, F. (2017) A global *Staphylococcus aureus* proteome resource applied to the *in vivo* characterization of host-pathogen interactions. *Sci. Rep. 7*, 9718.
(27) Palma Medina, L. M., Becker, A.-K., Michalik, S., Yedavally, H., Raineri, E. J. M., Hildebrandt, P., Gesell Salazar, M., Surmann, K., Pförtner, H., Mekonnen, S. A., Salvati, A., Kaderali, L., van Dijl, J. M., and Völker, U. (2019) Metabolic cross-talk between human bronchial epithelial cells and internalized Staphylococcus aureus as a driver for infection. *Mol. Cell. Proteomics 18*, 892−908.
(28) Surmann, K., Simon, M., Hildebrandt, P., Pförtner, H., Michalik, S., Stentzel, S., Steil, L., Dhople, V. M., Bernhardt, J., Schlüter, R., Depke, M., Gierok, P., Lalk, M., Bröker, B. M., Schmidt, F., and Völker, U. (2015) A proteomic perspective of the interplay of *Staphylococcus aureus* and human alveolar epithelial cells during infection. *J. Proteomics 128*, 203−217.
(29) Cozens, A. L., Yezzi, M. J., Kunzelmann, K., Ohrui, T., Chin, L., Eng, K., Finkbeiner, W. E., Widdicombe, J. H., and Gruenert, D. C. (1994) CFTR expression and chloride secretion in polarized immortal human bronchial epithelial cells. *Am. J. Respir. Cell Mol. Biol. 10*, 38−47.
(30) Ehrhardt, C., Kneuer, C., Laue, M., Schaefer, U. F., Kim, K.-J., and Lehr, C.-M. (2003) 16HBE14o- Human Bronchial Epithelial Cell Layers Express P-Glycoprotein, Lung Resistance-Related Protein, and Caveolin-1. *Pharm. Res. 20*, 545−551.
(31) Nagel, A., Michalik, S., Debarbouille, M., Hertlein, T., Salazar, M. G., Rath, H., Msadek, T., Ohlsen, K., van Dijl, J. M., Völker, U., and Mäder, U. (2018) Inhibition of Rho Activity Increases Expression of SaeRS-Dependent Virulence Factor Genes in *Staphylococcus aureus*, Showing a Link between Transcription Termination, Antibiotic Action, and Virulence. *mBio 9*, e01332-18.
(32) Matlin, K. S., Haus, B., and Zuk, A. (2003) Integrins in epithelial cell polarity: using antibodies to analyze adhesive function and morphogenesis. *Methods 30*, 235−246.
(33) Schoenenberger, C. A., Zuk, A., Zinkl, G. M., Kendall, D., and Matlin, K. S. (1994) Integrin expression and localization in normal MDCK cells and transformed MDCK cells lacking apical polarity. *J. Cell Sci. 107*, 527−541.
(34) Garzoni, C., and Kelley, W. L. (2009) *Staphylococcus aureus*: new evidence for intracellular persistence. *Trends Microbiol. 17*, 59−65.
(35) Monecke, S., Müller, E., Büchler, J., Stieber, B., and Ehricht, R. (2014) *Staphylococcus aureus In vitro* Secretion of Alpha Toxin (hla) Correlates with the Affiliation to Clonal Complexes. *PLoS One 9*, e100427.
(36) Horn, J., Stelzner, K., Rudel, T., and Fraunholz, M. (2018) Inside job: *Staphylococcus aureus* host-pathogen interactions. *Int. J. Med. Microbiol. 308*, 607−624.
(37) Wilke, G. A., and Wardenburg, J. B. (2010) Role of a disintegrin and metalloprotease 10 in *Staphylococcus aureus* α-hemolysin−mediated cellular injury. *Proc. Natl. Acad. Sci. U. S. A. 107*, 13473−13478.
(38) Pagels, M., Fuchs, S., Pané-Farré, J., Kohler, C., Menschner, L., Hecker, M., McNamarra, P. J., Bauer, M. C., von Wachenfeldt, C., Liebeke, M., Lalk, M., Sander, G., von Eiff, C., Proctor, R. A., and Engelmann, S. (2010) Redox sensing by a Rex-family repressor is involved in the regulation of anaerobic gene expression in *Staphylococcus aureus*. *Mol. Microbiol. 76*, 1142−1161.
(39) Somerville, G. A., and Proctor, R. A. (2009) At the Crossroads of Bacterial Metabolism and Virulence Factor Synthesis in Staphylococci. *Microbiol. Mol. Biol. Rev. 73*, 233−248.
(40) Luo, J., and Chen, A. F. (2005) Nitric oxide: a newly discovered function on wound healing. *Acta Pharmacol. Sin. 26*, 259.
(41) Lane, C., Knight, D., Burgess, S., Franklin, P., Horak, F., Legg, J., Moeller, A., and Stick, S. (2004) Epithelial inducible nitric oxide synthase activity is the major determinant of nitric oxide concentration in exhaled breath. *Thorax 59*, 757−760.
(42) Lee, W., and Thomas, P. S. (2009) Oxidative stress in COPD and its measurement through exhaled breath condensate. *Clin. Transl. Sci. 2*, 150−155.
(43) Liu, J., Sandrini, A., Thurston, M. C., Yates, D. H., and Thomas, P. S. (2007) Nitric oxide and exhaled breath nitrite/nitrates in chronic obstructive pulmonary disease patients. *Respiration 74*, 617−623.
(44) Malinovschi, A., Ludviksdottir, D., Tufvesson, E., Rolla, G., Bjermer, L., Alving, K., and Diamant, Z. (2015) Application of nitric oxide measurements in clinical conditions beyond asthma. *Eur. Clin. Respir. J. 2*, 28517.
(45) Akaike, T., and Maeda, H. (2000) Nitric oxide and virus infection. *Immunology 101*, 300−308.
(46) Bogdan, C. (2015) Nitric oxide synthase in innate and adaptive immunity: an update. *Trends Immunol. 36*, 161−178.
(47) Roy, S., Sharma, S., Sharma, M., Aggarwal, R., and Bose, M. (2004) Induction of nitric oxide release from the human alveolar epithelial cell line A549: an *in vitro* correlate of innate immune response to Mycobacterium tuberculosis. *Immunology 112*, 471−480.
(48) Löffler, B., Niemann, S., Ehrhardt, C., Horn, D., Lanckohr, C., Lina, G., Ludwig, S., and Peters, G. (2013) Pathogenesis of *Staphylococcus aureus* necrotizing pneumonia: the role of PVL and an influenza coinfection. *Expert Rev. Anti-Infect. Ther. 11*, 1041−1051.
(49) Herbert, S., Ziebandt, A.-K., Ohlsen, K., Schäfer, T., Hecker, M., Albrecht, D., Novick, R., and Götz, F. (2010) Repair of Global Regulators in *Staphylococcus aureus* 8325 and Comparative Analysis with Other Clinical Isolates. *Infect. Immun. 78*, 2877−2889.
(50) Liese, J., Rooijakkers, S. H. M., van Strijp, J. A. G., Novick, R. P., and Dustin, M. L. (2013) Intravital two-photon microscopy of host−pathogen interactions in a mouse model of *Staphylococcus aureus* skin abscess formation. *Cell. Microbiol. 15*, 891−909.

https://dx.doi.org/10.1021/acsinfecdis.0c00403
ACS Infect. Dis. 2020, 6, 2279−2290

(51) Pförtner, H., Wagner, J., Surmann, K., Hildebrandt, P., Ernst, S., Bernhardt, J., Schurmann, C., Gutjahr, M., Depke, M., Jehmlich, U., Dhople, V., Hammer, E., Steil, L., Völker, U., and Schmidt, F. (2013) A proteomics workflow for quantitative and time-resolved analysis of adaptation reactions of internalized bacteria. *Methods 61*, 244−250.
(52) van den Berg, S., Bonarius, H. P. J., van Kessel, K. P. M., Elsinga, G. S., Kooi, N., Westra, H., Bosma, T., van der Kooi-Pol, M. M., Koedijk, D. G. A. M., Groen, H., van Dijl, J. M., Buist, G., and Bakker-Woudenberg, I. A. J. M. (2015) A human monoclonal antibody targeting the conserved staphylococcal antigen IsaA protects mice against *Staphylococcus aureus* bacteremia. *Int. J. Med. Microbiol. 305*, 55−64.
(53) Bruderer, R., Bernhardt, O. M., Gandhi, T., Miladinović, S. M., Cheng, L.-Y., Messner, S., Ehrenberger, T., Zanotelli, V., Butscheid, Y., Escher, C., Vitek, O., Rinner, O., and Reiter, L. (2015) Extending the Limits of Quantitative Proteome Profiling with Data-Independent Acquisition and Application to Acetaminophen-Treated Three-Dimensional Liver Microtissues. *Mol. Cell. Proteomics 14*, 1400−1410.
(54) Fuchs, S., Mehlan, H., Bernhardt, J., Hennig, A., Michalik, S., Surmann, K., Pané-Farré, J., Giese, A., Weiss, S., Backert, L., Herbig, A., Nieselt, K., Hecker, M., Völker, U., and Mäder, U. (2018) AureoWiki- The repository of the *Staphylococcus aureus* research and annotation community. *Int. J. Med. Microbiol. 308*, 558−568.
(55) Ritchie, M. E., Phipson, B., Wu, D., Hu, Y., Law, C. W., Shi, W., and Smyth, G. K. (2015) limma powers differential expression analyses for RNA-sequencing and microarray studies. *Nucleic Acids Res. 43*, e47.
(56) R Core Team (2018) *R: A language and environment for statistical computing*, R Foundation for Statistical Computing, Vienna, Austria.

https://dx.doi.org/10.1021/acsinfecdis.0c00403
ACS Infect. Dis. 2020, 6, 2279−2290